2016 American Control Conference (ACC)
Boston Marriott Copley Place
July 6-8, 2016. Boston, MA, USA

Rational Iterative Feedforward Tuning: Approaches, Stable Inversion, and Experimental Comparison

Lennart Blanken, Frank Boeren, Dennis Bruijnen, Tom Oomen

***Abstract*— Feedforward control plays a key role in achieving high performance for industrial motion systems that perform non-repeating motion tasks. Recently, learning techniques have been proposed to further improve both performance and robustness to non-repeating tasks by using a rational feedforward basis. The aim of this paper is to propose a unifying framework which connects these approaches. Experimental results on an industrial motion system validate the approaches and illustrate benefits of rational feedforward tuning in motion systems, including pre- and post-actuation through stable inversion.**

I. INTRODUCTION

Feedforward control is essential for achieving performance requirements in industrial motion systems. The main performance improvement is often achieved by using feedforward of the reference. A common approach to feedforward control is model-based feedforward, in which a parametric model is exploited that approximates the inverse system. Typically, a parametric model of the plant is identified and inverted for use in feedforward [1]. However, the achievable performance is highly dependent on the model quality of the parametric model and the accuracy of the model inversion [2].

Iterative Learning Control (ILC) [3] can significantly improve performance of motion systems by learning from previous iterations. After each task, the feedforward signal for the next task is determined based on measured data and an approximate model of the system. However, extrapolation of the learned signal to other tasks often results in a significant performance deterioration, see, e.g., [4], [5]. This is highly undesired in industrial motion systems, which often perform non-repeating tasks, see, e.g., [6], [7].

To enable implementation on industrial motion systems, the following requirements are imposed on feedforward control: i) small servo error, and ii) high extrapolation capabilities with respect to non-repeating tasks. To enhance the extrapolation capabilities with respect to non-repeating tasks, segmented approaches to ILC are presented in [8], [9], [10], [11], where the task is divided into subtasks that are learned a priori. The use of such signal libraries can be restrictive since tasks are required to consist of previously learned subtasks. Instead of learning subtasks, polynomial basis functions are introduced in, e.g., [12], [13]. A rational parametrization of the feedforward controller is introduced in [14], [15], which enables high performance and extrapolation properties for the generic class of rational systems, i.e., systems that can be described by models containing both poles and zeros. These results significantly extend the polynomial parametrizations used in [12], [13]. These recent developments in ILC are promising for motion control with non-repeating tasks, yet still require an approximate model of the system.

Recently, an alternative approach to feedforward tuning is developed that enables estimation of feedforward controllers based on measured data only, denoted iterative feedforward control. An approach for a rational parameterization is proposed [16], whereas results for a polynomial parametrization are presented in [17], [18]. Interestingly, rational feedforward controllers enable pre-actuation through stable inversion, as is experimentally demonstrated in the present paper.

Although important theoretical steps have been made in iterative feedforward tuning, at present the connections and practical differences between different approaches are not yet fully understood. The contribution of this paper is twofold. First, a unifying formulation is proposed for iterative feedforward tuning approaches. Using this formulation, it is shown that iterative feedforward control, see [16], [17], [18], can be interpreted as norm-optimal ILC with basis functions, yet without the need for a model. Second, an experimental comparison is performed on an industrial motion system. Differences in the attainable performance are illustrated, and the proposed approach for pre-actuation is validated. In fact, the benefit of stable inversion can be clearly observed.

This paper is organized as follows. In Section II, the notation is introduced. In Section III, the feedforward control goal is outlined for high-precision motion systems and the necessity of parameterized feedforward is illustrated. Consequently, procedures for norm-optimal ILC and iterative feedforward tuning with rational parametrizations are proposed in Sections IV and V, respectively. In Section VI, an approach is proposed which enables pre- and post-actuation. In Section VII, results of the experimental comparison are presented. Finally, conclusions are provided in Section VIII.

II. PRELIMINARIES

A positive definite matrix A is denoted as $A \succ 0$, and $\|x\|_W^2 = x^\top W x$. All signals are often assumed to be of length N. Let $h(t)$ be the impulse response vector of a discrete-time, linear time-invariant (LTI), single-input, single output (SISO) system $\mathbf{H}(z)$. Then, the output y of the possibly noncausal $\mathbf{H}$ to input u is given by the truncated

L. Blanken, F. Boeren and T. Oomen are with the Eindhoven University of Technology, Dep. of Mechanical Engineering, Control Systems Technology Group, Eindhoven, The Netherlands. D. Bruijnen is with Philips Innovation Services, Mechatronics Technologies group, Eindhoven, The Netherlands. Email: l.l.g.blanken@tue.nl. This research is supported by Philips Innovation Services, the Innovational Research Incentives Scheme under the VENI grant Precision Motion: Beyond the Nanometer (no. 13073) awarded by NWO (The Netherlands Organisation for Scientific Research) and STW (Dutch Science Foundation).

978-1-4673-8681-4/$31.00 ©2016 AACC

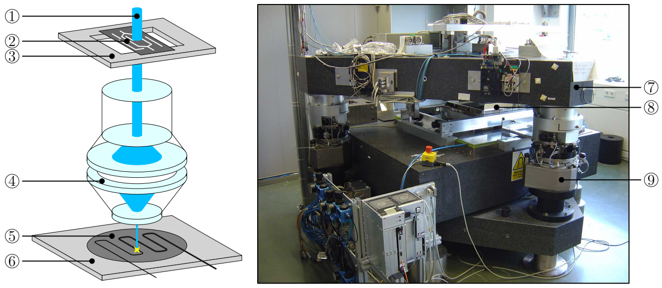

Fig. 1. Left: schematic illustration of a wafer scanner. Right: photograph of experimental wafer stage system. ①: light beam, ②: reticle, ③: reticle stage, ④: lens, ⑤: wafer, ⑥: wafer stage, ⑦: metrology frame, ⑧: mover, ⑨: airmount.

convolution

$$y(t) = \sum_{l=1-N}^{t} h(l)u(t-l),$$

where $0 \leq t < N$ and zero initial conditions are assumed. The finite-time convolution is denoted as

$$\underbrace{\begin{bmatrix} y(0) \\ y(1) \\ \vdots \\ y(N-1) \end{bmatrix}}_{y} = \underbrace{\begin{bmatrix} h(0) & h(-1) & \dots & h(1-N) \\ h(1) & h(0) & \dots & h(2-N) \\ \vdots & & \ddots & \vdots \\ h(N-1) & h(N-2) & \dots & h(0) \end{bmatrix}}_{H} \underbrace{\begin{bmatrix} u(0) \\ u(1) \\ \vdots \\ u(N-1) \end{bmatrix}}_{u}$$

with H the convolution matrix corresponding to $\mathbf{H}(z)$ and $u, y \in \mathbb{R}^N$ the input and output vectors.

III. FEEDFORWARD CONTROL GOAL

A. Experimental Setup

Wafer scanners are state-of-the-art opto-mechanical machines for producing integrated circuits (ICs) on a wafer [6], [7]. During the production process, an image of the desired IC pattern is exposed on the wafer. During exposure, the wafer stage performs a scanning motion with extreme accuracy. In addition, the reference profile varies between tasks to control the wafer height [6]. This high precision motion task imposes the following requirements on feedforward control:

R1. Small servo error.

R2. High extrapolation capabilities for non-repeating tasks.

Figure 1 depicts the considered industrial motion system. The stage is controlled in all six degrees of freedom (DOF), i.e., three translations and three rotations. Force actuators provide eight independent forces available for control, while laser interferometers enable subnanometer accuracy position measurements in all DOFs. A stabilizing multivariable feedback controller is determined by means of sequential loop-closing. The proposed feedforward approaches are applied to the main translational direction of motion.

B. Control Configuration

Figure 2 depicts the considered control setup, consisting of a stabilizing feedback controller C_{fb} and plant P. An identified frequency response function (FRF) of P is shown in Figure 3. Furthermore, r denotes the reference signal, e the measured error, f the feedforward signal, y the measured output, and v an unknown disturbance.

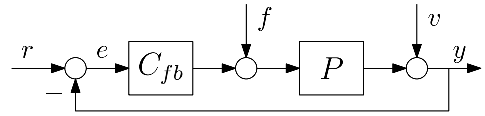

Fig. 2. Closed-loop control configuration.

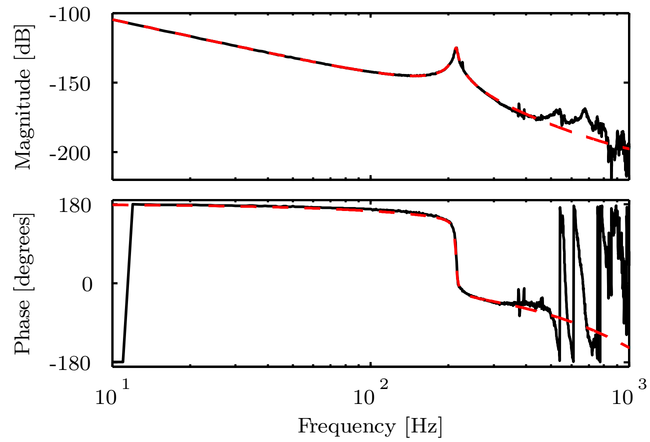

Fig. 3. FRF (——) of the plant P and model (– –) used by ILC.

C. Norm-Optimal ILC

Iterative Learning Control [3] is a proven method to improve the performance of a system subject to repeating tasks. In ILC, the feedforward signal is learned in a batch-to-batch fashion. A sequence of finite time tasks, denoted by index $j = 0, 1, 2, \ldots$, is performed under normal operating conditions. The feedforward f^{j+1} for task $j+1$ is determined by exploiting measured data from previous tasks and an approximate model $\widehat{SP}$ of SP, where $S = (I + PC_{fb})^{-1}$. In norm-optimal ILC, see, e.g., [3], [19], f^{j+1} is determined according to an optimization problem with criterion

$$V(f^{j+1}) = \|e^{j+1}(f^{j+1})\|_W^2, \tag{1}$$

where $W \succ 0$ is a user-defined weighting matrix, and the error propagation from task j to $j+1$ is given by

$$e^{j+1}(f^{j+1}) = e^j + \widehat{SP}\left(f^j - f^{j+1}\right).$$

This criterion can be directly extended by including weights on f^{j+1} and f^j as in, e.g., [3], [19]. To facilitate presentation, the form (1) is used.

A key advantage of ILC is the possibility to anticipate for all repeating disturbances under the assumption that the task is repeating [3]. However, non-repeating tasks in general result in a significant performance deterioration, see, e.g., [4], [5]. As a result, requirement R2 is not achieved by standard norm-optimal ILC. In this paper, the extrapolation capabilities of ILC are enhanced by parameterizing f^{j+1} in terms of basis functions, see, e.g., [12], [13], [14].

D. Feedforward Parameterization

The parametrization of f^{j+1} is important for the achievable performance and extrapolation capabilities with respect to non-repeating tasks. Existing approaches mainly focus on a polynomial parametrization, see, e.g., [13], [20], [21]. Extensions to a rational parametrization are presented in

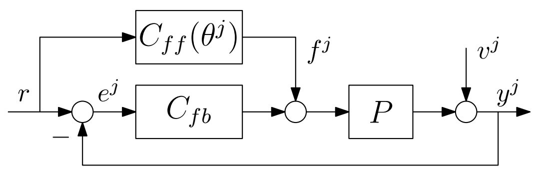

Fig. 4. The feedforward controller $C_{ff}(\theta^{j+1})$ is constructed based on measured signals in task j.

[14], [15], which showed potential to improve both performance and extrapolation capabilities. In this paper, a rational parametrization for C_{ff} is adopted to achieve both requirements R1 and R2. Let f^{j+1} be given by

$$f^{j+1} = C_{ff}(\theta^{j+1})r. \tag{2}$$

where $C_{ff}(\theta^{j+1})$ is parametrized as in Definition 1.

Definition 1. *The feedforward controller $C_{ff}(\theta)$ is parameterized in terms of a rational basis $\mathcal{C}_{rat}$, given by*

$$\mathcal{C}_{rat} = \left\{ C_{ff}(\theta) \middle| C_{ff}(\theta) = B(\theta)^{-1}A(\theta), \quad \theta \in \mathbb{R}^{n_a+n_b} \right\}$$

where

$$A(\theta) = \sum_{i=1}^{n_a} \psi_i \theta_i \qquad = \Psi_A \theta_A,$$

$$B(\theta) = I + \sum_{i=n_a+1}^{n_a+n_b} \psi_i \theta_i = I + \Psi_B \theta_B,$$

with $\theta = \begin{bmatrix} \theta_A \\ \theta_B \end{bmatrix}$ and basis functions $\Psi = \begin{bmatrix} \Psi_A, \Psi_B \end{bmatrix}$.

Here, ψ_i is the convolution matrix corresponding to polynomial basis function $\boldsymbol{\psi}_i(z)$. The underlying transfer function $\mathbf{C}_{ff}(\theta, z)$ of $C_{ff}(\theta)$ can be constructed as $\mathbf{C}_{ff}(z,\theta) = \mathbf{B}^{-1}(z,\theta)\mathbf{A}(z,\theta)$ where $\mathbf{A}(z,\theta) = \sum_{i=1}^{n_a} \boldsymbol{\psi}_i(z)\theta_i$ and $\mathbf{B}(z,\theta) = 1 + \sum_{i=n_a+1}^{n_a+n_b} \boldsymbol{\psi}_i(z)\theta_i$. Furthermore, a polynomial parameterization is recovered by setting $B(\theta) = I$.

E. Contribution of this Paper

For the parametrization in Definition 1, θ^{j+1} is determined according to the optimization problem

$$\theta^{j+1} = \arg\min_{\theta^{j+1}} V(\theta^{j+1}), \tag{3}$$

with criterion $V(\theta^{j+1})$ as defined next.

Definition 2. *The criterion for feedforward control with basis functions is given by*

$$V(\theta^{j+1}) = \|\hat{e}^{j+1}(\theta^{j+1})\|_W^2, \tag{4}$$

where $W \succ 0$ is a user-defined weighting matrix and $\hat{e}^{j+1}(\theta^{j+1})$ is a predicted error in task $j+1$.

The predicted error $\hat{e}^{j+1}(\theta^{j+1})$ depends on the selected approach, presented in Sections IV and V.

In this paper, approaches to solve (3) with $V(\theta^{j+1})$ in Definition 2 for $\mathcal{C}_{\text{rat}}$ in Definition 1 are presented and implemented on an industrial motion system. The contributions of this paper are as follows:

C1. (Section IV) Present a norm-optimal ILC approach for a rational basis, where a model of the system is used.
C2. (Section V) Present an iterative feedforward control approach for a rational basis, using measured data only.
C3. (Section VI) Stable inversion is employed to enable pre-actuation with rational feedforward controllers.
C4. (Section VII) Experimentally compare the approaches proposed in C1 and C2, and demonstrate the benefits of pre-actuation in C3 on an industrial motion system.

IV. NORM-OPTIMAL ILC WITH A RATIONAL BASIS

In this section, an approach is proposed to determine θ^{j+1} for norm-optimal ILC with a rational basis, as in [15]. Preliminary steps to this method can be found in [14]. The ILC update law for this approach is given by

$$\theta^{j+1}_{\langle k+1\rangle} = Q_{\text{ILC},\langle k\rangle}\theta^j + L_{\text{ILC},\langle k\rangle} e^j, \tag{5}$$

where the index k denotes the k^{th} computational iteration of an iterative scheme, and

$$L_{\text{ILC},\langle k\rangle} = \left[\left(\frac{\partial \hat{e}^{j+1}(\theta^{j+1}_{\langle k\rangle})}{\partial \theta^{j+1}_{\langle k\rangle}} \right)^{\top} W \Phi_{\text{ILC}}(\theta^{j+1}_{\langle k\rangle}) \right]^{-1} \cdot \left(\frac{\partial \hat{e}^{j+1}(\theta^{j+1}_{\langle k\rangle})}{\partial \theta^{j+1}_{\langle k\rangle}} \right)^{\top} W B^{-1}(\theta^{j+1}_{\langle k\rangle}) B^{-1}(\theta^j),$$

$$Q_{\text{ILC},\langle k\rangle} = L_{\text{ILC},\langle k\rangle} B(\theta^j)\Phi_{\text{ILC}}(\theta^j) \begin{bmatrix} I_{n_a} & 0 \\ 0 & -I_{n_b} \end{bmatrix}, \tag{6}$$

where 0 denotes the zero matrix of appropriate dimensions. For the parametrization in Definition 1, (5) follows from optimization problem (3) with $V(\theta^{j+1})$ in Definition 2, where for this approach $\hat{e}^{j+1}(\theta^{j+1})$ is given by

$$\hat{e}^{j+1}(\theta^{j+1}) = B^{-1}(\theta^{j+1})\tilde{e}^j - \Phi_{\text{ILC}}(\theta^{j+1})\theta^{j+1}, \tag{7}$$

with $\tilde{e}^j = e^j + \widehat{SP} f^j$ and regression matrix

$$\Phi_{\text{ILC}}(\theta^{j+1}) = B^{-1}(\theta^{j+1}) \begin{bmatrix} \widehat{SP}\Psi_A r, & -\Psi_B \tilde{e}^j \end{bmatrix}. \tag{8}$$

A derivation of (7) is omitted due to space restrictions.

For a polynomial parameterization of C_{ff}, i.e., $B(\theta) = I$, (5) equals the analytic solution given in [13], [22]. For a rational parametrization, (4) is in general nonlinear in θ^{j+1}. Typically, an iterative scheme is required, as provided next.

Procedure 1. Iterative scheme for rational ILC optimization

Given a model $\widehat{SP}$ of SP, θ^j and measured e^j in task j, set $k=0$ and initialize $\theta^{j+1}_{\langle 0\rangle} = \theta^j$. Then, perform the following sequence of steps to determine θ^{j+1}.

1) Initialize $L_{\text{ILC},\langle k\rangle}$ and $Q_{\text{ILC},\langle k\rangle}$ with $\theta^{j+1}_{\langle 0\rangle}$.
2) Determine $\theta^{j+1}_{\langle k+1\rangle} = Q_{\text{ILC},\langle k\rangle}\theta^j + L_{\text{ILC},\langle k\rangle} e^j$.
3) Construct $L_{\text{ILC},\langle k+1\rangle}$, $Q_{\text{ILC},\langle k+1\rangle}$, set $k \rightarrow k+1$ and return to 2) until an appropriate convergence condition is met.

V. IV-BASED ITERATIVE FEEDFORWARD CONTROL WITH A RATIONAL BASIS

In this section, an instrumental variable (IV) approach, see, e.g., [23], to feedforward control is presented and interpreted in a norm-optimal ILC framework. In contrast to ILC, no model $\widehat{SP}$ is required: the feedforward update is based on measured data only. This key difference potentially improves the convergence speed of the algorithm compared to norm-optimal ILC with basis functions, see Section VII-C. The proposed approach, recast as an ILC update law, is given by

$$\theta^{j+1}_{\langle k+1\rangle} = Q_{\mathrm{IV},\langle k\rangle}\theta^j + L_{\mathrm{IV},\langle k\rangle}e^j, \tag{9}$$

with

$$\begin{aligned} L_{\mathrm{IV},\langle k\rangle} &= \left[Z^\top(\theta^{j+1}_{\langle k\rangle})W\Phi_{\mathrm{IV}}(\theta^{j+1}_{\langle k\rangle})\right]^{-1} \\ &\quad\cdot Z^\top(\theta^{j+1}_{\langle k\rangle})WB^{-1}(\theta^{j+1}_{\langle k\rangle})B^{-1}(\theta^j), \\ Q_{\mathrm{IV},\langle k\rangle} &= L_{\mathrm{IV},\langle k\rangle}B(\theta^j)\Phi_{\mathrm{IV}}(\theta^j)\begin{bmatrix} I_{n_a} & 0 \\ 0 & -I_{n_b}\end{bmatrix}, \end{aligned}$$

where Z denotes the instrumental variables. Similar to (7), for this approach $\hat{e}^{j+1}(\theta^{j+1})$ is given by

$$\hat{e}^{j+1}(\theta^{j+1}) = B^{-1}(\theta^{j+1})\tilde{e}^j - \Phi_{\mathrm{IV}}(\theta^{j+1})\theta^{j+1}, \tag{10}$$

with $\tilde{e}^j = e^j + C_{ff}(\theta^j)C^{-1}y^j$, $C = C_{fb} + C_{ff}(\theta^j)$ and

$$\Phi_{\mathrm{IV}}(\theta^{j+1}) = B^{-1}(\theta^{j+1})\left[C^{-1}\Psi_A y^j, \quad -\Psi_B\tilde{e}^j\right]. \tag{11}$$

Comparing (11) with (8) shows that Φ_{IV} is fully based on measured data, while Φ_{ILC} contains an approximate model $\widehat{SP}$. This relies on the equivalence, see [21], of the relations

$$\begin{aligned} y^j &= \left(C_{fb} + C_{ff}(\theta^j)\right)SPr + Sv^j, \\ \left(C_{fb} + C_{ff}(\theta^j)\right)^{-1}y^j &= SPr, \end{aligned} \tag{12}$$

when assuming $v^j = 0$. Based on (12), measured data can be used to estimate SPr, eliminating the use of $\widehat{SP}$. By replacing $\widehat{SP}r$ in Φ_{ILC} with (12), Φ_{IV} in (11) is obtained. Furthermore, the gradient of (10) with respect to θ^{j+1} is

$$\begin{aligned} \frac{\partial\hat{e}^{j+1}(\theta^{j+1})}{\partial\theta^{j+1}} &= B^{-1}(\theta^{j+1})C^{-1} \\ &\quad\cdot\left[-\Psi_A y^j, \quad C_{ff}(\theta^{j+1})\Psi_B y^j\right]. \end{aligned} \tag{13}$$

Since both (11) and (13) contain measured data e^j and y^j, constructing L and Q as in (6) leads to biased estimates θ^{j+1}, see [18]. An IV-based solution is proposed in [18], where the instruments Z are designed to approximate (13) without using y^j. As a result, i) unbiased estimates are obtained, and ii) $V(\theta^{j+1})$ in (4) is approximately minimized upon convergence. The following instruments are proposed in [16]:

$$Z^\top(\theta^{j+1}_{\langle k\rangle}) = C^{-1}_{\langle k\rangle}\begin{bmatrix}\Psi_A r \\ -C_{ff}(\theta^{j+1}_{\langle k\rangle})\Psi_B r\end{bmatrix}, \tag{14}$$

with $C_{\langle k\rangle} = C_{fb} + C_{ff}(\theta^{j+1}_{\langle k\rangle})$. Similar to $\Phi_{\mathrm{IV}}(\theta^{j+1}_{\langle k\rangle})$, (14) depends on $\theta^{j+1}_{\langle k\rangle}$. Hence, an iterative procedure is required to refine (14), as in, e.g., [24]. This refinement can directly be included in the iterative scheme that is already required to determine θ^{j+1} for a rational parametrization, and is given next. For a polynomial parameterization of C_{ff}, i.e., $B(\theta) = I$, Procedure 2 is equal to the procedure given in [18].

Procedure 2. Iterative scheme for rational IV-based feedforward optimization

Given θ^j and measured e^j and y^j in task j, set $k = 0$ and initialize $\theta^{j+1}_{\langle 0\rangle} = \theta^j$. Then, perform the following sequence of steps to determine θ^{j+1}.

1) Initialize $Z(\theta^{j+1}_{\langle k\rangle})$, $L_{\mathrm{IV},\langle k\rangle}$ and $Q_{\mathrm{IV},\langle k\rangle}$ with $\theta^{j+1}_{\langle 0\rangle}$.
2) Determine $\theta^{j+1}_{\langle k+1\rangle} = Q_{\mathrm{IV},\langle k\rangle}\theta^j + L_{\mathrm{IV},\langle k\rangle}e^j$.
3) Construct $Z(\theta^{j+1}_{\langle k+1\rangle})$, $L_{\mathrm{IV},\langle k+1\rangle}$, $Q_{\mathrm{IV},\langle k+1\rangle}$, set $k \rightarrow k+1$ and return to 2) until a convergence condition is met.

VI. STABLE INVERSION

In this section, a stable inversion approach is presented to determine f^{j+1} in (2) for a rational feedforward controller. This approach relies on the assumption that r is known beforehand and is bounded, which is a typical assumption in motion systems. Let θ^{j+1} be determined according to update laws (5) or (9). Then, $C_{ff}(\theta^{j+1})$ follows from Definition 1 together with the underlying transfer function $\mathbf{C}_{ff}(\theta^{j+1}, z)$. If $\mathbf{C}_{ff}(\theta^{j+1}, z)$ is unstable, a bounded f^{j+1} can not be constructed when filtering forward in time. Next, a stable inversion approach is proposed to deal with unstable $\mathbf{C}_{ff}(\theta^{j+1}, z)$. Start by decomposing f^{j+1} into

$$f^{j+1} = \mathbf{C}^{\mathrm{st}}_{ff}(\theta^{j+1}, z)r + \mathbf{C}^{\mathrm{un}}_{ff}(\theta^{j+1}, z)r,$$

where $\mathbf{C}^{\mathrm{st}}_{ff}(\theta^{j+1}, z)$ and $\mathbf{C}^{\mathrm{un}}_{ff}(\theta^{j+1}, z)$ contain the stable and unstable dynamics, respectively. By means of stable inversion, see, e.g., [25], the unstable dynamics are filtered in backward time with suitable boundary conditions. As a result, a bounded f^{j+1} is computed. State-space expressions for LTI and LTV $\mathbf{C}^{\mathrm{st}}_{ff}(\theta^{j+1}, z)$ and $\mathbf{C}^{\mathrm{un}}_{ff}(\theta^{j+1}, z)$ are given in [18], [26].

The key benefit of stable inversion for feedforward is that pre-actuation is possible, i.e., the feedforward starts before the motion task. Simulation results have indicated that pre-actuation can potentially improve performance, see, e.g., [25], [27], [28]. In this paper, the benefits of stable inversion are demonstrated on the motion system in Figure 1. Pre- and post-actuation is clearly observed in Figure 9.

VII. EXPERIMENTAL COMPARISON

In this section, the iterative feedforward approaches of Sections IV and V and the stable inversion procedure in Section VI are demonstrated on the industrial motion system introduced in Section III. The experimental contributions are:

- The achievable performance of rational feedforward is compared to polynomial feedforward.
- The achievable performance of norm-optimal ILC and IV-based iterative feedforward control with rational bases is compared.
- The benefit of pre- and post-actuation for motion systems is demonstrated by means of stable inversion.

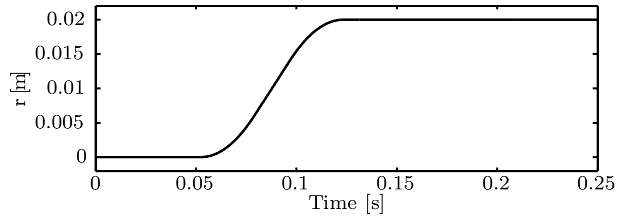

Fig. 5. Fourth order point-to-point reference signal r.

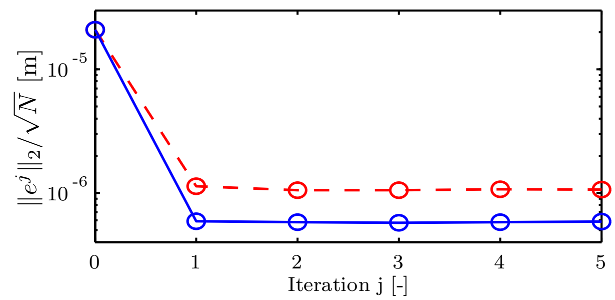

Fig. 6. The performance is improved significantly by the rational parameterization (-o-) compared to the polynomial parameterization (-o-).

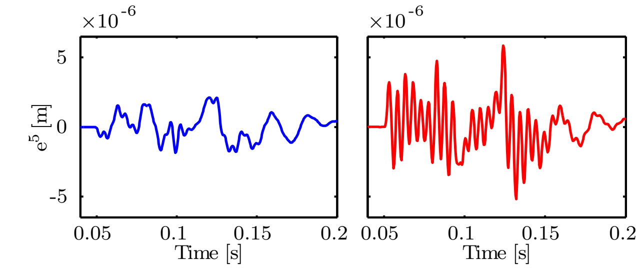

Fig. 7. The performance is improved significantly by the rational parameterization (—) compared to the polynomial parameterization (—).

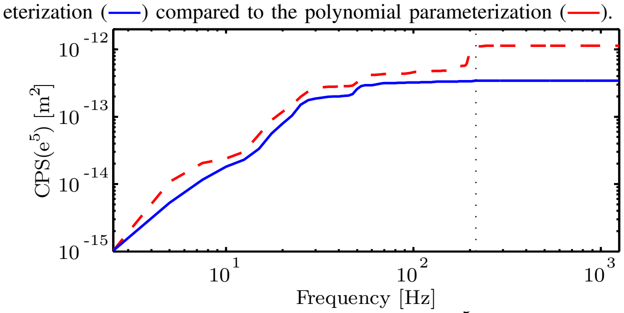

Fig. 8. The cumulative power spectrum (CPS) of e^5 shows that the dominant performance improvement of rational feedforward (—) compared to polynomial feedforward (– –) is obtained around the first flexible mode of the plant at approximately 220 Hz.

A. Experiment Setup

The control goal for the considered motion system described in Section III-A is to minimize $\|e^j\|^2$, with r a fourth order motion task, depicted in Figure 5, and y^j the measured position of the system. All signals operate in discrete time with sample time $T_s = 1/2500$ s. The basis functions used for the polynomial parametrization are given by

$$\Psi_A(z) = \left[\frac{z-1}{zT_s}, \left(\frac{z-1}{zT_s}\right)^2, \left(\frac{z-1}{zT_s}\right)^3, \left(\frac{z-1}{zT_s}\right)^4, \left(\frac{z-1}{zT_s}\right)^5\right],$$

corresponding with differentiators, as in, e.g., [14], [18], [29]. The rational parameterization in Definition 1 is given by

$$\Psi_A(z) = \left[\frac{z-1}{zT_s}, \quad \left(\frac{z-1}{zT_s}\right)^2, \quad \left(\frac{z-1}{zT_s}\right)^4, \quad \left(\frac{z-1}{zT_s}\right)^5\right],$$

$$\Psi_B(z) = \left[\frac{z-1}{zT_s}, \quad \left(\frac{z-1}{zT_s}\right)^2, \quad \left(\frac{z-1}{zT_s}\right)^3\right].$$

Note that the selection of the bases is non-trivial. For the polynomial basis, these basis functions facilitate an intuitive physical interpretation of the parameters. E.g., the parameter corresponding to $\left(\frac{z-1}{zT_s}\right)^2$ is the estimated mass of the system.

B. Rational vs. Polynomial

In this section, the influence is investigated of the feedforward parameterization on the performance. To this purpose, the IV-based iterative feedforward control approaches in Section V are compared with rational and polynomial bases. Similar experimental results for norm-optimal ILC with basis functions are omitted for brevity. The results are shown in Figures 6 to 9, where the following observations are made:

- Rational feedforward improves performance by 50% in terms of $\|e^j\|^2$ compared to polynomial feedforward.
- Both procedures converge in a single task, see Figure 6.

The performance enhancement of rational feedforward is contributed to the following aspects.

- The dominant performance improvement of rational feedforward is achieved in the frequency range $180 - 220$ Hz, see Figure 8. The enhanced flexibility of the rational basis enables compensation for the first flexible mode of the plant, whereas this is not achieved by the polynomial basis.
- Figure 9 demonstrates pre-actuation, used to prevent transient errors at the start of the motion task, and post-actuation, used to reduce residual vibrations in the system. This feature is key for the potential performance improvement of rational feedforward compared to polynomial feedforward. Resulting effects can be observed in Figure 7.

To further improve performance, the following is proposed.

- Figures 7 and 8 indicate that a low frequent contribution up to 60 Hz is not compensated for by the feedforward. This is contributed to nonlinearities in the system and the cable slab between the fixed world and the stage, acting as a low-frequency disturbance. Inclusion of these dynamics in the designed basis functions is a topic for future work.

C. IV-Based Feedforward Control vs. Norm-Optimal ILC

In this section, norm-optimal ILC and IV-based feedforward control with rational bases are compared, see Sections IV and V. The parametric model of the system used by ILC is depicted in Figure 3. The experimental results are shown in Figure 10. The following observations are made:

- The ILC procedure requires multiple tasks to converge, due to the use of model $\widehat{SP}$. As a consequence, the performance after one task is significantly compromised.
- The iterative feedforward procedure converges in one task, validating the use of (12) in update law (9).
- After convergence, both approaches achieve similar performance.

VIII. CONCLUSIONS

In this paper, two approaches are presented for learning of rational feedforward controllers: i) norm-optimal ILC using a model, and ii) IV-based iterative feedforward control using only measured data. Both approaches enable high performance and extrapolation capabilities for non-repeating tasks. Experimental results on an industrial motion system

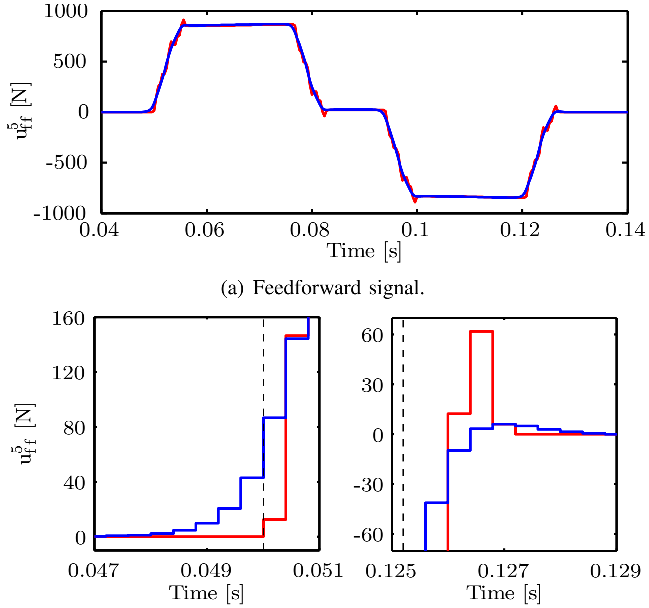

(a) Feedforward signal.

(b) Pre-actuation. (c) Post-actuation.

Fig. 9. The rational parameterization (——) enables pre- and post-actuation of the system, in contrast to the polynomial parametrization (——). The start and end times of the motion task are indicated by black dashed lines.

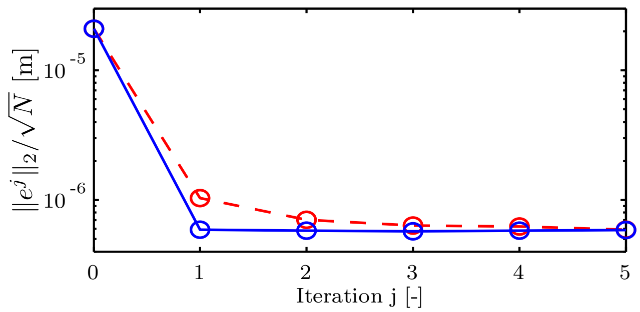

Fig. 10. The convergence speed of ILC (–○–) is compromised due to the model quality of $\widehat{SP}$, compared to iterative feedforward control (–○–). After convergence, similar performance is obtained.

validate the approaches, and illustrate benefits of rational feedforward: i) improved performance compared to polynomial feedforward, and ii) possible pre- and post-actuation by means of stable inversion. Ongoing research focuses on extensions to multivariable, position-dependent, and time-varying systems [26], possibly in an inferential control context [30].

REFERENCES

[1] J. Butterworth, L. Pao, and D. Abramovitch, "Analysis and comparison of three discrete-time feedforward model-inverse control techniques for nonminimum-phase systems," *Mechatronics*, vol. 22, no. 5, pp. 577–587, 2012.

[2] S. Devasia, "Should model-based inverse inputs be used as feedforward under plant uncertainty?" *IEEE Trans. Automat. Contr.*, vol. 47, no. 11, pp. 1865–1871, 2002.

[3] D. Bristow, M. Tharayil, and A. Alleyne, "A survey of iterative learning control," *IEEE Control Syst. Mag.*, vol. 26, no. 3, pp. 96–114, 2006.

[4] D. Hoelzle, A. Johnson, and A. Alleyne, "Bumpless transfer filter for exogenous feedforward signals," *IEEE Trans. Contr. Syst. Technol.*, vol. 22, no. 4, pp. 1581–1588, 2014.

[5] S. Mishra and M. Tomizuka, "Projection-based iterative learning control for wafer scanner systems," *IEEE/ASME Trans. Mechatron.*, vol. 14, no. 3, pp. 388–393, 2009.

[6] H. Butler, "Position control in lithographic equipment," *IEEE Control Syst. Mag.*, vol. 31, no. 5, pp. 28–47, 2011.

[7] T. Oomen, R. van Herpen, S. Quist, M. van de Wal, O. Bosgra, and M. Steinbuch, "Connecting system identification and robust control for next-generation motion control of a wafer stage," *IEEE Trans. Contr. Syst. Technol.*, vol. 22, no. 1, pp. 102–118, 2014.

[8] S. Mishra, J. Coaplen, and M. Tomizuka, "Precision positioning of wafer scanners segmented iterative learning control for nonrepetitive disturbances," *IEEE Control Syst. Mag.*, vol. 27, no. 4, pp. 20–25, 2007.

[9] D. Hoelzle, A. Alleyne, and A. Johnson, "Basis task approach to iterative learning control with applications to micro-robotic deposition," *IEEE Trans. Contr. Syst. Technol.*, vol. 19, no. 5, pp. 1138–1148, 2011.

[10] H. Wang, K. Kim, and Q. Zou, "B-spline-decomposition-based output tracking with preview for nonminimum-phase linear systems," *Automatica*, vol. 49, no. 5, pp. 1295 – 1303, 2013.

[11] H. Wang and Q. Zou, "B-spline-decomposition-based approach to multiaxis trajectory tracking: Nanomanipulation example," *IEEE Trans. Contr. Syst. Technol.*, vol. 22, no. 4, pp. 1573–1580, July 2014.

[12] M. Q. Phan and J. Frueh, "Learning control for trajectory tracking using basis functions," in *Proceedings of the 35th IEEE Conference on Decision and Control*, 1996, pp. 2490–2492.

[13] J. van de Wijdeven and O. Bosgra, "Using basis functions in iterative learning control: analysis and design theory," *Int. J. Control*, vol. 83, no. 4, pp. 661–675, 2010.

[14] J. Bolder, T. Oomen, and M. Steinbuch, "Rational basis functions in iterative learning control - with experimental verification on a motion system," *IEEE Trans. Contr. Syst. Technol.*, vol. 23, no. 2, pp. 722–729, 2015.

[15] J. van Zundert, J. Bolder, and T. Oomen, "Iterative learning control for varying tasks: Achieving optimality for rational basis functions," in *Proceedings of the 2015 American Control Conference*, Chicago, IL, USA, 2015, pp. 3570–3575.

[16] F. Boeren, L. Blanken, D. Bruijnen, and T. Oomen, "Optimal estimation of rational feedforward controllers: An instrumental variable approach," in *Proceedings of the 54th IEEE Conference on Decision and Control*, Osaka, Japan, 2015, pp. 6058–6063.

[17] F. Boeren, T. Oomen, and M. Steinbuch, "Accuracy aspects in motion feedforward tuning," in *Proceedings of the 2014 American Control Conference*, Portland, OR, USA, 2014, pp. 2178–2183.

[18] ——, "Iterative motion feedforward tuning: A data-driven approach based on instrumental variable identification," *Contr. Eng. Prac.*, vol. 37, pp. 11 – 19, 2015.

[19] S. Gunnarsson and M. Norrlöf, "On the design of ILC algorithms using optimization," *Automatica*, vol. 37, no. 12, pp. 2011–2016, 2001.

[20] M. Heertjes, D. Hennekens, and M. Steinbuch, "MIMO feed-forward design in wafer scanners using a gradient approximation-based algorithm," *Contr. Eng. Prac.*, vol. 18, no. 5, pp. 495 – 506, 2010.

[21] S. van der Meulen, R. Tousain, and O. Bosgra, "Fixed structure feedforward controller design exploiting iterative trials: Application to a wafer stage and a desktop printer," *J. Dyn. Syst. Meas. Control*, vol. 130, no. 5, pp. 0 510 061–05 100 616, 2008.

[22] J. A. Frueh and M. Q. Phan, "Linear quadratic optimal learning control (LQL)," *Int. J. Control*, vol. 73, no. 10, pp. 832–839, 2000.

[23] T. Söderström and P. Stoica, *Instrumental Variable Methods for System Identification*, ser. Lecture Notes in Control and Information Sciences. Springer-Verlag, Berlin, Germany, 1983, vol. 57.

[24] P. Young, "Refined instrumental variable estimation: Maximum likelihood optimization of a unified Box-Jenkins model," *Automatica*, vol. 52, pp. 35 – 46, 2015.

[25] T. Sogo, "On the equivalence between stable inversion for nonminimum phase systems and reciprocal transfer functions defined by the two-sided Laplace transform," *Automatica*, vol. 46, no. 1, pp. 122 – 126, 2010.

[26] J. van Zundert, J. Bolder, S. Koekebakker, and T. Oomen, "Resource-efficient ILC for LTI/LTV systems through LQ tracking and stable inversion: Enabling large feedforward tasks on a position-dependent industrial printer," 2016, submitted for journal publication.

[27] S. Devasia, "Time-optimal control with pre/post actuation for dual-stage systems," *IEEE Trans. Contr. Syst. Technol.*, vol. 20, no. 2, pp. 323–334, 2012.

[28] Q. Zou, "Optimal preview-based stable-inversion for output tracking of nonminimum-phase linear systems," *Automatica*, vol. 45, no. 1, pp. 230 – 237, 2009.

[29] P. Lambrechts, M. Boerlage, and M. Steinbuch, "Trajectory planning and feedforward design for electromechanical motion systems," *Contr. Eng. Prac.*, vol. 13, no. 2, pp. 145 – 157, 2005.

[30] T. Oomen, E. Grassens, and F. Hendriks, "Inferential motion control: Identification and robust control framework for positioning an unmeasurable point of interest," *IEEE Trans. Contr. Syst. Technol.*, vol. 23, no. 4, pp. 1602–1610, July 2015.